https://ntrs.nasa.gov/search.jsp?R=19670022951 2020-03-12T11:17:32+00:00Z

FACILITY FORM 602
N67-32280 (ACCESSION NUMBER)
54 (PAGES)
CR-72269 (NASA CR OR TMX OR AD NUMBER)
(THRU) 1
(CODE)
06 (CATEGORY)

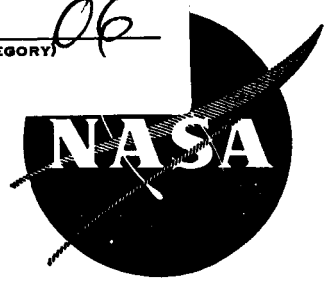

NASA CR 72269

EXPLORATORY STUDIES OF CONTACT ANGLE HYSTERESIS, WETTING OF SOLIDIFIED RARE GASES AND SURFACE PROPERTIES OF MERCURY

by

Anthony M. Schwartz, Alfred H. Ellison,
John D. Galligan and Charles A. Rader

Prepared for

National Aeronautics and Space Administration

May 19, 1967

GPO PRICE $ _____

CFSTI PRICE(S) $ _____ Contract NAS 3-8909

Hard copy (HC) 3.00

Microfiche (MF) .65

ff 653 July 65

GILLETTE RESEARCH INSTITUTE, INC.
6220 Kansas Avenue, N.E., Washington, D.C. 20011

NOTICE

This report was prepared as an account of Government sponsored work. Neither the United States, nor the National Aeronautics and Space Administration (NASA), nor any person acting on behalf of NASA:

A.) Makes any warranty or representation, expressed or implied, with respect to the accuracy, completeness, or usefulness of the information contained in this report, or that the use of any information, apparatus, method, or process disclosed in this report may not infringe privately owned rights; or

B.) Assumes any liabilities with respect to the use of, or for damages resulting from the use of any information, apparatus, method or process disclosed in this report.

As used above, "person acting on behalf of NASA" includes any employee or contractor of NASA, or employee of such contractor, to the extent that such employee or contractor of NASA, or employee of such contractor prepares, disseminates, or provides access to, any information pursuant to his employment or contract with NASA, or his employment with such contractor.

Requests for copies of this report should be referred to

National Aeronautics and Space Administration
Office of Scientific and Technical Information
Attention: AFSS-A
Washington, D. C. 20546

NASA CR 72269

Final Report

EXPLORATORY STUDIES OF CONTACT ANGLE HYSTERESIS, WETTING OF SOLIDIFIED RARE GASES AND SURFACE PROPERTIES OF MERCURY

by

Anthony M. Schwartz, Alfred H. Ellison,
John D. Galligan and Charles A. Rader

Prepared for

National Aeronautics and Space Administration

Contract NAS 3-8909

Technical Management
NASA Lewis Research Center
Cleveland, Ohio
Spacecraft Technology Division
Edward W. Otto

GILLETTE RESEARCH INSTITUTE, INC.
6220 Kansas Avenue, N.E., Washington, D.C. 20011

EXPLORATORY STUDIES OF CONTACT ANGLE HYSTERESIS, WETTING OF SOLIDIFIED RARE GASES AND SURFACE PROPERTIES OF MERCURY

By Anthony M. Schwartz, Alfred H. Ellison,
John D. Galligan and Charles A. Rader

Abstract

Three new areas of fundamental surface chemistry were explored in this work. These were: new approaches to contact angle hysteresis, the wetting of solidified rare gas surfaces and the effect of trace metal impurities on the surface properties of mercury. In the contact angle hysteresis work systems were studied in which surface roughness and/or chemical heterogenity were eliminated or controlled so as to obtain evidence for "intrinsic" hysteresis. In the second phase of the work, Argon, Krypton, and Xenon were condensed as solid films on metal planchets at suitable temperatures and the spreading of suitable liquids on the surfaces observed. In the third phase of the work, the effect of trace impurities on the surface properties of mercury was observed by changes in the appearance, wetting by liquids, and surface potential.

SUMMARY

The work reported here comprised three exploratory investigations of new fundamental areas of surface chemistry. The object was to obtain exploratory data and to define areas for further study.

In Task I, the objective was to demonstrate the existence of "intrinsic" factors contributing to contact angle hysteresis by new approaches in which heterogeneity both physical and chemical were eliminated or controlled. Contact angle hysteresis was found to be absent where all of the phases were low viscosity fluids. When one of the phases was a high viscosity fluid such as polyethylene at its softening point, large contact angle hysteresis was observed but this may be a non-equilibrium condition. When one of the phases was a rigid solid such as polished diamond, substantial hysteresis was observed in spite of the fact that light interference measurements showed this surface to be smooth and flat. Hysteresis was found to be negligible in the contact angles of water on monolayers on mercury. These results along with recently published reports in the literature regarding the effect of adsorption on contact angles strongly suggest that physical heterogeneity or roughness is not the only factor in contact angle hysteresis and that hysteresis may also be caused by "intrinsic" factors related to adsorption.

In Task II, the object was to observe contact angles of suitable liquids on solids in which intermolecular forces were of the simplest type. Thus, the rare gases Argon, Krypton, and Xenon were condensed as solid films on metal planchets at suitable temperatures and their wetting

by suitable liquids was observed. The number of liquids available for contact angle observations on the three rare gas solids was limited severely by the temperature requirements of the experiments. Thus, with Argon (m.p. 84° K), Nitrogen (b.p. 78° K), was used as the refrigerant and the only liquid available at this temperature was Oxygen (m.p. 55° K; b.p. 91° K), which spread on the solid Argon. Since liquid Oxygen has a surface tension of approximately 18 dynes/cm one can conclude that the critical surface tension, γ_c , is greater than 18 dynes/cm. Krypton (m.p. 116° K) was condensed with Nitrogen as the refrigerant in which case Oxygen was the only liquid available and it spread on the solid Krypton. Krypton was also condensed with methane as the refrigerant (b.p. 112° K) in which case ethane (m.p. 90°; b.p. 185° K), butene (m.p. 88° K; b.p. 267° K) and Freon 14 (m.p. 89° K; b.p. 145° K) were suitable liquids; however, all dissolved the solid Krypton obviating contact angle measurements. The only conclusion possible, therefore, is that the critical surface tension of solid Krypton at 78° K is greater than 18 dynes per centimeter. Xenon (m.p. 161° K) was condensed with liquid nitrogen as the refrigerant in which case liquid oxygen was found to spread on it also. Xenon was also condensed to a solid with methane as the refrigerant (b.p. 112° K) in which case ethane was found to dissolve the solid Xenon as it had the solid Krypton. However when Xenon was condensed with Freon 14 (b.p. 145° K) two liquids, allyl alcohol (m.p. 144° K; b.p. 370° K) and ethane thiol (m.p. 125° K; b.p. 308° K) formed contact angles with the solid Xenon. Unexpectedly, the contact angle of ethane

thiol on solid Xenon was smaller than the contact angle of allyl alcohol in spite of the fact that the latter had the lower surface tension. No explanation for this reversal in the contact angle surface tension relationship was found. Thus, the critical surface tension of solid Xenon is greater than 18 dynes/cm at 78° K and less than 36 dynes/cm at 145° K.

The Task III work involved the effect of trace metal impurities upon the surface properties of Mercury. A fresh surface of Mercury undergoes a change with time that was followed by the spreading of water and benzene on the surface and by the relative surface potential. After a period of time the surface appears to become static as characterized by no further changes in the spreading characteristics of water and benzene or of the surface potential. These wetting and surface potential properties both the change with time and the final equilibrium values are greatly affected by the presence of trace amounts, such as 2 ppm of Zinc and Lead; Gold had no effect. The effect is almost immediate upon application of the contaminant. The changing surface properties appear to be due to the adsorption of gas molecules on the surface for which the impurities act as a catalyst or to the presence of impurity molecules in the surface.

INTRODUCTION

Previous work for the Spacecraft Technology Division of the NASA Lewis Research Center carried out at the Gillette Research Institute involved the determination of contact angle data of selected liquids on selected solids for application to the zero gravity problem of spacecraft tank design. (1) With this work completed, it was decided to explore some new areas of fundamental surface chemistry of probable future interest to NASA. Three areas were selected: new approaches to the study of contact angle hysteresis, contact angles on solidified rare gas surfaces and the study of the effect of trace metal impurities upon the surface properties of Mercury. These comprised three separate tasks and are reported as such below.

In addition to the writers the following people contributed to this work: Mr. George A. Lyerly, Mr. Bernard Kidda, and Mr. R. Bruce Klemm.

MATERIALS

Methylene iodide - Fisher Scientific Co., purified

Water - Double distilled

Perfluorokerosene - Peninsular Chemresearch, Inc., low boiling fraction

n-Hexadecane - Eastman Organic Chemicals Co., practical

Vistanex-Polyisobutylene - Enjay Chemical Co., Vistanex LMMS

Polyethylene glycol 400 - Fisher Scientific Co., U.S.P.

Polyethylene - Allied Chemical Co., Grade 1702

Tricresyl phosphate - Fisher Scientific Co., technical grade

Polytetrafluoroethylene - "Teflon"

Diamond - Industrial diamond approx. 1 cm x 0.8 cm x 0.2 cm thick. Borrowed for this work from W. A. Zisman and E. G. Shafrin of the Naval Research Laboratories, Washington, D. C.

Methanol - Fisher Scientific Co., reagent grade

Tide - Procter and Gamble Co., Inc.

Freon 113 - duPont fluorocarbon solvent

Mercury - Fisher Scientific Co., instrument grade

Dodecanoic acid - Eastman Organic Chemical Co., white label grade

Tetradecanoic acid - Eastman Organic Chemical Co., white label grade

Hexadecanoic acid - Fisher Scientific Co., reagent grade

Octadecanoic acid - Armour and Co., Research Division, research grade

Eicosanoic acid - Eastman Organic Chemical Co., white label grade

1 - Tetradecanol - Eastman Organic Chemical Co., white label grade

1 - Hexadecanol - Fisher Scientific Co., N. F.

Materials, continued:

1 - Octadecanol - Eastman Organic Chemical Co., white label grade

Liquid nitrogen - Air Products, Inc.

Argon - Air Products, Inc.

Krypton - Matheson, Inc., research grade

Xenon - Matheson, Inc., research grade

Ethane - Matheson, Inc., research grade

Propane - Matheson, Inc., research grade

Butene - Matheson, Inc., research grade

Methane - Matheson, Inc., commercial grade

Freon 14 - Matheson, Inc., 95% by volume

Allyl alcohol - Fisher Scientific Co., reagent grade

Ethanethiol - Eastman Organic Chemical Co., white label grade

Allyl chloride - Eastman Organic Chemical Co., white label grade

Nitric oxide - Matheson, Inc., 99.5% by volume

Nitrogen gas - Air Products, Inc., ultra high purity grade

Benzene - Fisher Scientific Co., reagent grade

Gold - Fisher Scientific Co., purified

Zinc - Fisher Scientific Co., sticks

Lead - Fisher Scientific Co., #8 shot

TASK I - CONTACT ANGLE HYSTERESIS

A. INTRODUCTION

Contact angles of liquids on solids usually show hysteresis, that is, the angle is larger if measured following an advance of the liquid over the solid than if measured following a recession of the liquid over the solid. For many years contact angle hysteresis was attributed entirely to surface roughness (2). More recently other causes have been proposed (3 - 5). It was the object of this phase of the work to obtain additional experimental evidence for these other contact angle hysteresis factors particularly for the "intrinsic" factor proposed by Schwartz, Rader, and Huey (5). To do this, contact angles were measured in systems where surface roughness was not a factor. Thus advancing and receding contact angles were observed: in all fluid systems, as a function of temperature in solid/liquid systems wherein roughness was a constant, on a polished surface of diamond which was shown to be smooth and flat by light interference techniques, and on spread organic monolayers on mercury.

B. EXPERIMENTAL

Two experimental techniques were common to all four approaches. The first was in the measurement of the contact angle by the "NRL (Naval Research Laboratory) contact angle goniometer." One modification of it was made because of the peculiar requirements of this work. The telescope was mounted on a micro manipulator so that it could be moved transversely

so as to view both sides of a drop in contact with a substrate without moving the contact angle system. This was necessary since movement of the contact angle system as is customary in contact angle measurements by the NRL contact angle goniometer would cause vibrations in the contact angle system, probably resulting in a change in the advancing angle or receding angle.

The other technique common to all of the hysteresis work was also related to vibrations in the contact angle system. The syringes used to deliver liquid drops in the contact angle systems were kept in contact with the drop during the measurements of advancing and receding angles since to withdraw the syringe tip from the drop would cause a vibration of the drop and a change in the advancing or receding angle.

Special techniques peculiar to the four approaches to the contact angle hysteresis work will be described in the appropriate sections.

C. PROCEDURES AND RESULTS

1. Contact Angle Hysteresis In All Fluid Systems

Liquid surfaces are homogeneous; thus, it was of value to observe the advancing and receding angles in all fluid systems. The first system studied was methylene iodide/water/air. This system was chosen because it had been studied by previous workers using a different method and the results would serve as a check on our experimental set-up. Drops of the two liquids were formed on the tips of syringes and brought into contact in the field of the goniometer telescope. The system was photographed as

shown in Figure 1 and the contact angle through air measured from the photograph. To determine an advancing angle the syringe tips were brought closer together to increase the interfacial area or additional liquid was added to the drops also increasing interfacial area. Both methods gave the same result. Receding contact angles were obtained by reversing the procedure.

Although the angle measured in these systems was the angle through air it can easily be shown that if this angle does not change the angles in the other two phases also do not change.

When the results checked with literature values additional systems were investigated. These were hexadecane/perfluorokerosene/air and hexadecane/perfluorokerosene/water. The results are summarized in Table I. It can be seen that no contact angle hysteresis is observed in these all fluid systems.

The next series of all fluid systems chosen for study were: Vistanex/water/air, Vistanex/polyethylene glycol 400/air and polyethylene/ polyethylene glycol 400/air. Vistanex is a highly viscous polyisobutylene which at room temperature is a glassy near-solid material. Polyethylene glycol 400 is a relatively low viscosity liquid. Polyethylene is of course a solid at room temperature; however, at 118° C it undergoes a transition to a glassy semi-solid similar to but more viscous than Vistanex. These systems were chosen to investigate the transition region between liquid/ liquid systems which show no contact angle hysteresis and liquid/solid systems which show substantial contact angle hysteresis.

The experimental set-up used for these contact angle measurements is shown in Figure 2. The glassy semi-solid was either a polyethylene planchet cut from rodstock and given a smooth flat surface by pressing against a glass surface heated to the softening point of the polyethylene, or a Teflon cup filled to the brim with Vistanex. The specimens were placed in a jacketed optical cell for temperature control and drops of the polyethylene glycol 400 were delivered to these surfaces from a microsyringe.

No quantitative contact angle data were obtained for the systems containing Vistanex because the water or polyethylene glycol 400 tended to sink into the Vistanex surface and no steady state contact angle was observed.

With the polyethylene/polyethylene glycol 400/air system advancing and receding contact angles were observed at room temperature and at intervals up to the softening point of the polyethylene. The results are summarized in Table II. It can be seen that the same moderate amount of contact angle hysteresis is observed from 25 to 100° C. However, as the polyethylene planchet undergoes a transition from an opaque white solid to a glassy semi-solid when the air temperature in the cell is 118° contact angle hysteresis increases. Attempts were made to continue the observations to higher temperatures with the idea that the viscosity of the polyethylene would decrease and the contact angle hysteresis would disappear. However, the viscosity of the polyethylene decreased only slowly as the temperature was further raised and it showed signs of chemical decomposition before the desired low viscosity could be reached.

When drops of polyethylene glycol 400 were left in contact with polyethylene at 118° for long periods of time and then removed a depressed area on the surface of the polyethylene could be seen where the liquid drop had been resting. This suggested that the data reported in Table II might not be equilibrium data even though no distortion of the polyethylene surface could be detected in the time period of these experiments. Since the data for the systems involving a highly viscous phase may not be equilibrium data the large hysteresis observed, although highly interesting, must be labeled as an anamolous effect.

2. The Effect of Temperature on Contact Angle Hysteresis

The "intrinsic" hysteresis factor concept incorporates the idea of a layer of immobilized adsorbed liquid molecules on the solid surface. The possibility therefore existed that increasing the temperature would increase the mobility of this layer and reduce hysteresis. It was of course not known at what temperature mobility could be produced; thus these experiments would be significant only if a positive result was obtained. That is, if increasing the temperature caused a decrease in hysteresis good evidence for an intrinsic factor would be obtained; however, if increasing the temperature did not decrease the hysteresis this would not necessarily rule out the intrinsic factor.

The following systems were used to observe the effect of temperature on contact angle hysteresis: tricresylphosphate/Teflon/air, methylene iodide/Teflon/air and water/Teflon/air. The results are summarized in Table III. It can be seen that contact angle hysteresis does not change with temperature; in fact, it is remarkably constant

3. Contact Angle Hysteresis on Polished Diamond

The availability of a highly polished industrial diamond made possible the observation of contact angle hysteresis on a highly smooth and flat surface. The smoothness and flatness of this surface was verified by light interference techniques using the Do-All apparatus.

Cleaning methods for the diamond surface involving abrasion or washing with strong cleaning acids had to be avoided since they would probably destroy the smoothness of the surface. Alternative solvent treatments may sometimes leave residues in which case the homogenity of the surface would be in question. It was, therefore, decided to clean the surface using three mild cleaning agents with the idea that if residues were left they could be detected by measurement of water contact angles. Contact angle results for the three cleaning procedures are shown in Table IV. Since essentially the same advancing and receding contact angle for water on diamond was obtained after each of the three cleaning procedures it is concluded that no residues are left and the angles are actually diamond/water/air angles. It is also to be noted that there was substantial contact angle hysteresis of the water contact angle.

Table V summarizes contact angle data for water, glycerine, and methylene iodide on a polished diamond surface. These data show that substantial contact angle hysteresis is observed with liquids other than water. Although there is still the possibility of a certain amount of surface heterogenity even with this highly smooth and flat diamond surface

the data do point strongly to the existence of other causes of contact angle hysteresis.

Since to our knowledge this was the first contact angle data on diamond a Zisman plot of the data was made. This is shown in Figure III and indicates a critical surface tension value of 40.4 dynes per cm.

4. Hysteresis of Contact Angles of Water on Monolayers on Mercury

Contact angles of water on monolayers of straight chain polar materials such as stearic acid on solid substrates show hysteresis (3, 6). In these studies the contribution to the hysteresis of surface roughness could not be assessed because of the difficulty of defining the roughness of a solid surface. By studying hysteresis of water contact angles on monolayers spread on mercury, two objectives would be accomplished. First, the unknown effect of substrate roughness would be eliminated and, second, the hysteresis could be studied as a function of molecular packing in the monolayer. The latter requires that the film be spread in a mercury film balance (7).

A line drawing showing the principal components of the apparatus is shown in Figure 4. The apparatus is a commercially available Cenco hydrophil balance with a lucite plastic insert to reduce the volume of mercury necessary to fill the trough and also to prevent contact between the mercury and the metal trough. A surface barrier and float system of 1 mil Mylar film as described by Ellison (7) is used. Figure 4 shows the micropipette with a capillary delivery tip attached to a micro

manipulator, the goniometer telescope, and the lamp for illuminating the contact angle system. In a typical experiment, the mercury surface is swept clean with surface barriers on both sides of the balance float, the monolayer is spread from benzene solution on the left hand side of the balance float and then the water contact angle, film pressure and film area are recorded at intervals as the film is compressed.

In this work, it was necessary to know that the water drop was sitting on the monolayer and did not displace the monolayer and sit on the mercury. The following shows how this was accomplished.

First, it is necessary to understand the compressional characteristics or the surface pressure-area relationship for these monolayers on mercury. All of the n-alkyl acids and alcohols, from C_{12} to C_{20} show the same type of pressure-area curve. This is shown in Figure 5. As these films are compressed, the curve of surface pressure vs. area per molecule reflects first a packing of the molecules in a horizontal orientation, i.e., lying flat on the surface; and then a constant pressure region in which the molecules are presumed to be reorienting to the vertical orientation (7); and then a second increase in pressure associated with packing of the molecules in the vertical orientation. The response of the contact angle in the constant pressure region of the pressure-area curve labeled π_c is indicative of whether the monolayer is interposed between the water and the mercury or not. The two cases are shown schematically in Figure 6. In case 1 where the monolayer is interposed between the water and the mercury the contact angle changes as the molecules pack together and present a surface of increasing hydrophobicity.

In case 2 the water is not sitting on the monolayer but rather on the mercury surface and the contact angle is determined by the piston film action of the monolayer surrounding it. Since in this region the pressure is constant the contact angle does not change.

As indicated above, both types of behavior were observed. Figure 7 shows the cosine θ - pressure and cosine θ - area relationships for the stearic acid monolayer. It can be seen that this is case 2. Cosine θ, and of course θ also, is constant in the πc region. Also, in the cosine θ - film pressure plot there is no indication of a changing contact angle at the constant pressure, πc. With tetradecanoic acid, however, the corresponding curves shown in Figure 8 show a change in cosine θ, and therefore θ, as the molecular packing changes in the critical pressure region and likewise a change in cosine θ at the critical pressure point in the cosine θ - film pressure relationship. This is case 1.

The behavior of the homologous C_{12}, C_{14}, C_{16}, C_{18} and C_{20} acids as well as that of the C_{14}, C_{16} and C_{18} alcohols was observed. It was found that in both series the C_{16} and higher members followed the case 2 behavior while the C_{14} and lower members followed the case 1 behavior. A very probable explanation of the difference in behavior of the lower and higher members of these series is the displacing ability of the materials relative to water. A possible measure of this is the equilibrium spreading pressure, πe, of the materials. The equilibrium spreading pressure of a material is the spontaneous spreading pressure generated by a

monolayer in equilibrium with an excess of the material at a given temperature. This is a two dimensional analog of vapor pressure. This was measured for the various n-alkyl alcohols and acids and found, as expected, to increase with a decrease in molecular weight. The measured values are summarized in Table 6. Since the C_{14} acid and alcohol displace water and the C_{16} homologs do not, we would expect the equilibrium spreading pressure for water to lie between the equilibrium pressures of these two materials. Our method of measuring equilibrium spreading pressure, placing an amount of the material in excess of the monolayer amount on the clean surface of mercury in a film balance and observing the pressure generated, cannot be used for volatile materials such as water. We therefore searched the literature and found two values reported and these are given in Table 6. The agreement between these two values is satisfactory considering the difficulty of the measurement. The value that would be predicted on the basis of our relative displacement picture would lie between these two literature values. This is considered good support for the relative displacement explanation.

Since good reasons have been given for believing that the water droplet sits on a tetradecanoic acid monolayer on mercury we can use this system for our contact angle hysteresis measurement. When this was done negligible, less than 2°, hysteresis was observed in the water contact angle over a wide range of molecular packing. Although no contact angle hysteresis was observed in these experiments a negative result is inconclusive. Apparently even the close packed monolayer of tetradecanoic

acid on mercury is not solid or sufficiently solid to immobilize the first layer of water in contact with it.

D. DISCUSSION

The work with the all fluid systems of low viscosity shows that in the absence of physical and chemical surface heterogeneity, contact angle hysteresis is also absent. The work on the effect of temperature on contact angle hysteresis failed to provide evidence for an "intrinsic" factor but such negative evidence is inconclusive. Contact angles of water on monolayers on mercury also failed to provide evidence for an "intrinsic" hysteresis factor but again such negative evidence is inconclusive.

The large hysteresis observed in the contact angles of liquids on a polished surface of diamond is strong evidence for an "intrinsic" factor. The surface of this diamond was highly smooth and flat according to the light interference observations and since it is a single crystal its surface should be nearly homogeneous from the chemical standpoint. Since recent literature (8) supports the view of a strongly adsorbed monolayer of the liquid on the solid in a liquid/solid system showing a finite contact angle, it is very probable that a large hysteresis in the contact angle of liquids on polished diamond was caused at least in part by an "intrinsic" factor.

E. CONCLUSION

Clear, unambiguous experimental evidence for an "intrinsic" factor in contact angle hysteresis was not found; however, strong support for an "intrinsic" factor is provided by the large hysteresis observed in the contact angles of liquids on polished diamond.

TASK II. THE WETTING OF SOLIDIFIED RARE GASES

A. INTRODUCTION

A theory which permits calculation of solid surface energy is available. The application of this theory to the surface energy of solidified rare gases has been made and the results should be accurate because of the relatively simple interatomic forces involved (9). The calculated surface energies were in the range 16-42 $\frac{ergs}{cm^2}$ A theoretical comparison has been drawn between solid surface energy and critical surface tension (10). However additional experimental data is needed. Thus the object of this Task II work was to obtain data on the critical surface tension of solidified rare gases.

The rare gases chosen for study were those that could be solidified with the readily available refrigerant, liquid nitrogen, and also presented no hazard. These, then, were Argon, Krypton, and Xenon. The search for commercially available materials that were liquid at boiling nitrogen temperature produced only one material, oxygen. Thus it was necessary to work at higher temperatures where possible and experiments were done with Krypton at boiling methane temperature and with Xenon at boiling Freon 14 temperature. Ethane, 1-butene, nitric oxide, and Freon 14 are suitable for wetting Krypton at boiling methane temperature. Allyl alcohol, ethanethiol, and allyl chloride are liquid at boiling Freon 14 temperature.

B. PROCEDURES AND RESULTS

A polished steel planchet was cooled to the desired temperature in an inert atmosphere, and the given rare gas was introduced by means of a delivery tube terminating just above the surface of the planchet. In a short time a solid film of the rare gas was visible on the surface of the steel planchet. The delivery tip for the rare gas was removed and replaced with a similar one for delivery of the liquid whose contact angle was to be observed. This material liquified in the delivery tube and fell gently on the solidified rare gas surface. The apparatus for carrying out these experiments is shown in Figure 9.

The first experiments were done with liquid nitrogen as the refrigerant. It was thought that the temperature of the steel planchet in this apparatus would be a few degrees higher than the refrigerant thus permitting a contact angle observation with propane. However, when propane was added to the surface it solidified instantly. The only easily available liquid for wetting studies at liquid nitrogen temperature proved to be oxygen, which remains liquid at temperatures well below the boiling point of nitrogen. Oxygen was therefore used as the test liquid in the above experiment. It spread to zero contact angle on all three solidified rare gas surfaces.

The next group of experiments was done with methane as the refrigerant. A supply of liquid methane was obtained by passing the gas over a cold finger chilled with liquid nitrogen and collecting the liquid methane in a Dewar flask. The liquids available at methane temperature

were ethane, propane, butene, nitric oxide, and Freon 14. The spreading of each of these except nitric oxide was observed on Krypton and Xenon but valid contact angles could not be obtained because these liquids attacked, that is, dissolved, the solid Krypton and Xenon surfaces. Nitric oxide did not condense as a liquid but deposited on the cell walls as a white frosty solid containing blue patches. This behavior suggests that it reacted with residual oxygen in the system to form a mixture of nitrogen dioxide combined with the nitric oxide.

The next material used as a refrigerant was Freon 14. Although some additional hydrocarbons were liquids at Freon 14 temperature they were not used because it was expected that they would be solvents for the solid Xenon. Polar liquids were sought and three were found. These were: allyl alcohol, allyl chloride, and ethanethiol. The allyl chloride was found to be a good solvent for the Xenon; however, allyl alcohol and ethane thiol did not wet nor attack the Xenon surface and their contact angles were measured. All of the spreading results are summarized in Table 7.

C. DISCUSSION

This exploratory work showed that it is entirely feasible to condense rare gases as solid films and observe their wetting by suitable liquids. In the relatively simple apparatus used, however, where temperatures were limited by the availability of a suitable refrigerant the number of liquid/solid contact angle systems that could be studied was extremely small. In a more elaborate apparatus, however, comprising

perhaps heaters and temperature controllers, temperatures intermediate between those of the refrigerant liquids could be obtained and this would make available several more liquids.

A surprising result was that the contact angles of ethane thiol and allyl alcohol on solid Xenon were in the reverse of what would be expected on the basis of their surface tensions. The contact angles were double-checked as were the surface tensions. In the latter case, the surface tension values that were determined checked very closely with those calculated from surface tension values at higher temperature taken from the literature. Thus no explanation can at present be offered for the reversal in the contact angles.

On the basis of the limited data available it can be said that the critical surface tensions of Argon, Krypton, and Xenon are greater than 18 dynes per cm at 78° K. Further, the critical surface tension of Xenon at 145° K is less than 36 dynes per cm.

D. CONCLUSION

The calculated surface energies of the solid rare gases are in the range 16 - 42 $\frac{ergs}{cm^2}$ (9). The critical surface tensions estimated from the contact angle data reported above are of this magnitude but more accurate data would be necessary to test the hypothesis of identity between critical surface tension and surface energy.

TASK III. THE EFFECT OF IMPURITIES UPON UPON THE SURFACE PROPERTIES OF MERCURY

A. INTRODUCTION

It has been reported (11) that the formation of visible surface films or scum on liquid mercury is related to the presence of dissolved metallic impurities in mercury. Previous work showed that such a surface film interfered with film balance studies of organic monolayers on mercury (7). It is possible that this surface film would also affect the wetting of solids by mercury as reported in an earlier NASA report (1).

The experimental objective was to observe the changes in the wetting properties and surface potentials of mercury upon addition of trace amounts of metals. Thus the spreading of water and benzene on pure and trace metal contaminated mercury was studied. Surface potential measurements on these mercury surfaces were made by the radioactive electrode technique.

B. EXPERIMENTAL

The attainment of the objective of this work required that reagent grade materials be used, that the experiments be carried out in a controlled, reproducible atmosphere, and that all apparatus contacting the mercury be clean with respect to both organic and inorganic or metallic residues.

A small rectangular Pockels trough with a capacity of about 500 g Hg was fabricated from Plexiglas. Trough frame pieces and sweeping barriers were made from 0.001" Mylar film after Fahir (12) and Ellison (7) and were supported by brass bars. This apparatus with the below described surface potential measuring electrode in place is shown in Figure 10.

Small liquid drops (.005 ml or 5λ) were applied to the mercury surfaces from micropipettes.

Surface potentials were measured after Bewig (13), using a radium ionization electrode obtained from U. S. Radium Corporation and a Kiethley Model 610 B electrometer coupled to a Sargent Model MR potentiometric recorder. An Eppley Cat. No. 100 standard cell provided a calibration voltage.

The mercury trough was cleaned prior to each run by rinsing with strong nitric acid, followed by copious amounts of distilled water.

For observations of liquid spreading, the trough was filled with mercury, its surface swept, and the spreading liquids were applied to the mercury surface as a series of drops at time intervals. Several types of spreading behavior were observed. The first, referred to below simply as "spreading," was when a small droplet of liquid spread to a large, flat lens; and, as it evaporated, interference fringes formed around the periphery of the drop. Since the droplets quickly evaporated, successive testings of the mercury surface could be made as close as 15 seconds apart initially after sweeping. A second stage referred to below as "low drop" was when the drop formed a low contact angle with the mercury surface but did not spread further and never displayed interference fringes. The third stage referred to below as "high drop" was when a high contact angle drop was observed when liquid was touched to the mercury surface.

For surface potential observations, the Pockels trough was filled with mercury, the surface was swept, and the surface potential recorded as a function of surface aging time.

Impurities were added to mercury in the trough predissolved in 1 ml of mercury to form 2 ppm solutions in the trough.

The mercury was cleaned for re-use by acid washing, followed by distillation after Gordon and Wichers (11).

C. RESULTS

1. Water and benzene spreading

The spreading behavior of water and benzene on freshly swept distilled mercury surfaces changed as the surface aged after sweeping. Table VIII summarizes the observations for both liquids on distilled mercury and on mercury containing 2 ppm dissolved trace metal (Au, Pb, or Zn) impurities. The spreading behavior of mercury containing 2 ppm Au apparently paralleled that of distilled mercury. The effect of 2 ppm Pb in the mercury was to reduce the time that both water and benzene would continue to spread on a freshly swept surface. The benzene result was contradictory in that benzene did not form a high drop up to 20 minutes' surface aging, whereas the high drop did form at 20 minutes' surface aging on distilled mercury. This contradiction suggests that the lead contaminated mercury surface reached some equilibrium, whereas the distilled mercury surface continued to change. No spreading was observed for either water or benzene on the zinc contaminated mercury surface, although benzene showed a low drop initially.

2. Surface Potentials

The spreading experiments indicated that some surface change occurred upon aging and it was desirable to characterize this change by other means. A continuous observation of the changing surface was desirable. Measurement of the surface potential was chosen for this purpose. The effect of surface aging on surface potential is shown in Figure 11 for distilled and contaminated mercury. The Figure shows that there is a change in potential with the surface aging of each mercury system. The potential reaches a virtually constant value within several minutes, the exact time depending on the specific system. Although both liquid spreading and surface potential show that the surfaces change with time, it is apparently not true that any particular degree of wettability is associated with any particular potential.

Another way to demonstrate the effect of added metal impurity on the surface potential of mercury, which also indicates the time response, is to add the impurity to uncontaminated mercury while recording the potential. The results of this type of experiment are shown in Figure 12. The freshly swept surface of uncontaminated mercury was allowed to age until the steady surface potential was reached, and then the contaminant metal, predissolved in a small amount of mercury at a concentration to give 2 ppm. after addition, was added. The addition was made to a region of the mercury surface separated by a surface barrier from the region where the surface potential was being measured, so that the contaminant could not reach this latter region by diffusing along the surface. The results show that the surface potential responds

rapidly to the addition of zinc; thus the surface potential changes by about 0.800 volts within about one minute following the addition of the zinc. When lead was added to the mercury, a similar result was obtained. A negligible change in potential was observed following the addition of gold.

When the zinc contaminated mercury surface was swept to observe surface aging (Figure 11), a lower potential (+0.225V) was obtained. Sweeping the surface of lead or gold contaminated mercury solutions gave no significant change in the observed potential.

3. Mercury Surface Appearance

The surface luster of all the mercury systems was the same and no visible changes of the undisturbed surfaces occurred upon aging. However, upon sweeping, it was apparent that surface films had formed on the mercury surfaces to an extent dependent on the contaminant. In the case of lead- or zinc-contaminated mercury, the slightest compression of the surface by means of the sweeping barrier caused visible wrinkling. With distilled mercury and gold contaminated mercury, a slight, greyish powdery residue collected in front of the sweeping barrier, but no coherent surface film was formed as was noted in the case of zinc- and lead-contaminated mercury. Repeated sweeping of the surface of zinc-contaminated mercury caused a gradual diminution in the amount of surface film collected. With lead-contaminated mercury, the amount of surface film collected with repeated sweeping appeared not to diminish. However, it is possible that the same effect would occur with lead as with zinc,

if a greater number of sweeps were used. Observations on liquid spreading and potential were consistent with the visual observations. Thus, repeated sweeping of zinc-contaminated mercury surfaces causes these properties to change in a direction towards clean mercury. Also in keeping with the visual observations, these surface properties of lead-contaminated mercury showed no observable change with repeated surface sweeping.

D. DISCUSSION

The change in the observed surface properties of uncontaminated mercury with time is believed to involve an equilibration of the fresh surface with the gas phase rather than an equilibration from a dynamic to static surface. Thus, some component (or components) of the gas phase could be adsorbing on the mercury surface and changing the wetting and surface potential properties. Although the gas phase in these experiments was nominally dry nitrogen, no conclusion can be reached regarding the adsorbed component since even extremely low concentrations of less inert components, such as oxygen, carbon dioxide, and possibly volatile organic matter, could provide sufficient material to rapidly saturate the mercury surface.

The important observation made in this work is that certain metallic impurities in trace amounts have a large effect on the observed surface properties. Whether the effect on surface properties is due solely to the adsorption of the metal impurity atoms at the mercury/gas interface

or a combination of metal impurity adsorption and gas adsorption cannot be deduced from the presently available data. That adsorption of the metal impurity atoms actually occurs is shown by the fact that repeated surface sweeping of zinc-contaminated mercury gradually eliminates the effect of the zinc. A comparison of the non-swept surface potential curve shown in the final portion of Figure 12 (after the addition of zinc), with the swept surface potential curve shown in Figure 11 (Zn, 2 ppm) illustrates the sweeping effect. The adsorbed metal impurity atoms could be adsorption sites for gas phase components or they could be catalysts for the adsorption of gas phase components on surface mercury atoms or both.

The "pure" or uncontaminated mercury used in this work was purified to a very high degree. However, it may still contain some trace impurities. Since the addition of 2 ppm. of zinc or lead has such a large effect, it would appear that the level of such "active" trace impurities would be somewhat below the ppm level. It is therefore possible that even more highly purified mercury might remain hydrophilic for a longer period of time and have a different surface potential.

The spreading experiments indicate that the surface of both uncontaminated mercury and contaminated mercury become non-wettable by water and benzene, the difference being that the contaminated mercury becomes non-wettable in a much shorter time. It is evident that a film forms on the surface in both cases. On the other hand, the final steady state surface potential of the uncontaminated and contaminated mercury are very different. This indicates that the two films may differ chemically

as well as physically. Additional work is necessary to resolve these questions.

E. CONCLUSION

Certain metal impurities in trace quantities exert a large effect on the surface properties of mercury. The behavior can be likened to the behavior of surfactants in water.

BIBLIOGRAPHY

1. A. M. Schwartz and A. H. Ellison, NASA Report No. CR-54708 of Contract NAS 3-7104, Jan. 13, 1966

   G. A. Lyerly and H. Peper, NASA Report No. CR-54175 of Contract NAS 3-5744, Dec. 31, 1964

2. R. N. Wenzel, Ind. Eng. Chem. 28, 988 (1936)

3. C. O. Timmons and W. A. Zisman, J. Colloid Interface Sci. 22, 165 (1966)

4. R. E. Johnson, Jr. and R. H. Dettre, Adv. Chem. Series. 43, 112 (1964)

   R. H. Dettre and R. E. Johnson, Jr. ibid, 136

   R. E. Johnson, Jr. and R. H. Dettre, J. Phys. Chem. 68, 1744 (1964)

   R. H. Dettre and R. E. Johnson, Jr., ibid, 69, 1507 (1965)

5. A. M. Schwartz, C. A. Rader and E. Huey, Adv. Chem. Series 43, 250 - 267 (1964)

6. L. S. Bartell and R. J. Ruch, J. Phys. Chem. 60, 1231 (1956)

7. A. H. Ellison, J. Phys. Chem. 66, 1867 (1962)

8. A. W. Adamson, L. Dormant, and M. Orem, An Adsorption Theory of Contact Angle and Spreading, presented at National ACS meeting, Miami Beach, Fla., April 9 - 14, 1967

9. G. L. Pollack, Rev. Modern Physics, 36, 748 (1964)

10. M. C. Phillips and A. C. Riddiford, Z. Physik. Chem. Neue Folge, Bd. 47, S. 17 - 19 (1965)

11. C. L. Gordon and E. Wickers, Ann. N. Y. Assd. Sci. 65, 369 - 87 (1957)

12. E. Fahir, J. Chim. Phys. 27, 587 (1930)

13. K. W. Bewig, Rev. Sci. Instr. 35, (9), 1160-62 (1964)

TABLE I

ADVANCING AND RECEDING CONTACT ANGLE MEASUREMENTS

System	Equil. Contact Angles		
	Advancing Degrees	Receding Degrees	Hysteresis Degrees
Methylene iodide/water/air	150	150	0
Perfluorokerosene/ Hexadecane/air	175	174	1
Perfluorokerosene/ Hexadecane/water	166	164	2

TABLE II

EFFECT OF TEMPERATURE ON CONTACT ANGLE HYSTERESIS

FOR THE POLYETHYLENE/POLYETHYLENE GLYCOL 400/AIR SYSTEM

Temperature °C	Contact Angles		Hysteresis Degrees
	Advancing, Degrees	Receding, Degrees	
25	56	51	5
50	56	50	6
75	59	51	8
100	61	51	10
118	62	51	11
118	66	46	20
118	65	35	30
118	68	24	44

TABLE III

EFFECT OF TEMPERATURE ON CONTACT ANGLE HYSTERESIS

System	Equilibrium Contact Angles			
	Temperature (°C)	Advancing (degrees)	Receding (degrees)	Hysteresis (degrees)
Poly(tetrafluoroethylene)/ Tricresyl Phosphate/air	25	76	54	22
	50	78	54	24
	75	78	53	25
	100	78	53	25
	125	79	55	24
	150	81	56	25
Poly(tetrafluoroethylene)/ Methylene Iodide/air	25	90	62	28
	50	90	64	26
	75	90	64	26
	100	90	64	26
Poly(tetrafluoroethylene)/ water/air	25	118	98	20
	50	117	98	19
	75	117	96	21
	90	118	96	22

TABLE IV

EFFECT OF CLEANING AGENT ON WATER CONTACT ANGLES ON POLISHED DIAMOND

Cleaning Agent	Equilibrium Contact Angles		
	Advancing (degrees)	Receding (degrees)	Hysteresis (degrees)
Tide	53	21	32
Methanol	59	26	33
Freon 113	59	27	32

TABLE V

EQUILIBRIUM CONTACT ANGLES FOR VARIOUS LIQUIDS

ON POLISHED DIAMOND CLEANED WITH MEHTANOL

	Equilibrium Contact Angles		
Liquids	Advancing (degrees)	Receding (degrees)	Hysteresis (degrees)
Water	59	26	33
Glycerol	49	20	29
Methylene Iodide	33	21	12

TABLE VI

EQUILIBRIUM SPREADING PRESSURE ON

MERCURY AT 25°C

Material	(dynes/cm)
Water (Harkins)	>32
Water (Kemball)	46
Dodecanoic Acid	44.5
1-Tetradecanol	41.5
Tetradecanoic Acid	42
1-Hexadecanol	39
Hexadecanoic Acid	40
1-Octadecanol	35
Octadeconoic Acid	35
Eicosanoic Acid	32

TABLE VII

THE WETTING OF SOLID NOBLE GASES BY LIQUIDS

Solid/Refrigerant/Temperature (°K)	Liquid	Melting Point (°K)	Boiling Point (°K)	Surface Tension (dynes/cm)	Advancing Contact Angle (degrees)
Argon/Nitrogen/78°	Oxygen	55	91	18[1]	Spread
Krypton/Nitrogen/78°	Oxygen	55	91	18[1]	Spread
Xenon/Nitrogen/78°	Oxygen	55	91	18[1]	Spread
Krypton/Methane/112°	Ethane	89.9	184.7	28.08[3]	Spread[2]
Krypton/Methane/112°	1-Butene	87.8	268	--	Spread[2]
Krypton/Methane/112°	Nitric Oxide	109.6	--	--	--[4]
Krypton/Methane/112°	Freon-14	89.2	145	--	Spread[2]
Xenon/Methane/112°	Ethane	89.9	184.7	28.08[3]	Spread[2]
Xenon/Freon-14/145°	Allyl Alcohol	144	170	38[5],38[8]	94
Xenon/Freon-14/145°	Ethanethiol	125	308	44[6],43[8]	46
Xenon/Freon-14/145°	Allyl Chloride	139	318	41[7]	Spread[2]

---

1. Baly and Donnan, J. Chem. Soc. (London), 81, 907 (1902) (at 70°K).
2. These liquids attacked the solid surface, apparently dissolving it.
3. American Petroleum Institute publication Research Project 44 (extrapolated).
4. Nitric oxide did not form a liquid, but condensed as a solid.
5. H. Roland and M. Fels; Bull. Soc. Chim. Belg. 40, 177-94 (1931) (extrapolated).
6. W. E. Haines et al; J. Phys. Chem. 58, 370-78 (1954) (extrapolated).
7. Am. Chem. Soc., Adv. Chem. Ser. 29; Physical Properties of Chemical Compounds III, p. 277 (extrapolated).
8. Measure at this laboratory at 145°K.

TABLE VIII

THE SPREADING OF WATER AND BENZENE ON CLEAN AND CONTAIMINATED MERCURY

Mercury System	Liquid	Initial Effect	Time to "Low Drop"[1]	Time to "High Drop"[2]
Distilled	water	spreading	2 min.	2.5 min.
	benzene	"	19 min.	20 min.
2 ppm. Au	water	"	2 min.	2.5 min.
	benzene	"	19 min.	20 min.
2 ppm. Pb	water	"	30 sec.	6 min.
	benzene	"	7 min.	> 20 min.[3]
2 ppm. Zn	water	high drop	--	--
	benzene	low drop	--	2 min.

1. Low contact angle drop.

2. High contact angle drop.

3. The low contact angle drop persisted and the experiment was terminated after 20 minutes.

FIGURE 1

Liquid/Liquid/Air Contact Angle Apparatus

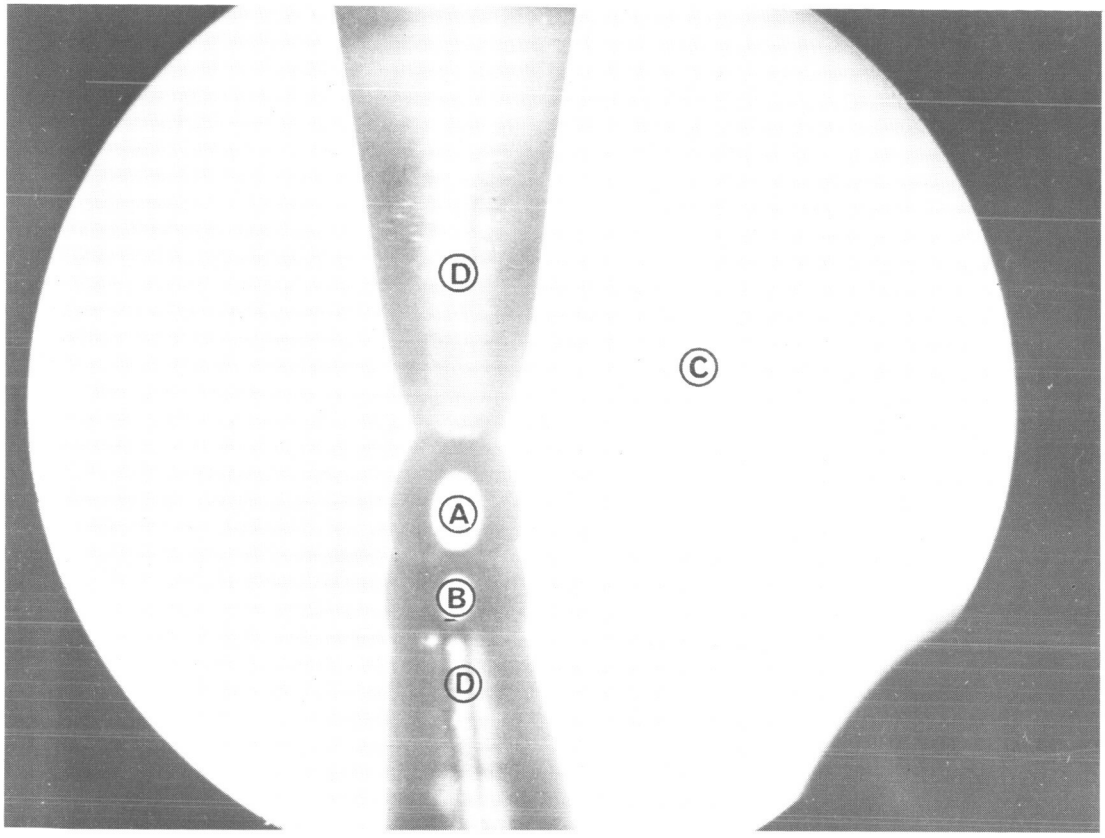

A - Water
B - Methylene Iodide
C - Air
D - Syringe Tips

FIGURE 2

Semi-solid/Liquid/Air Contact Angle Apparatus

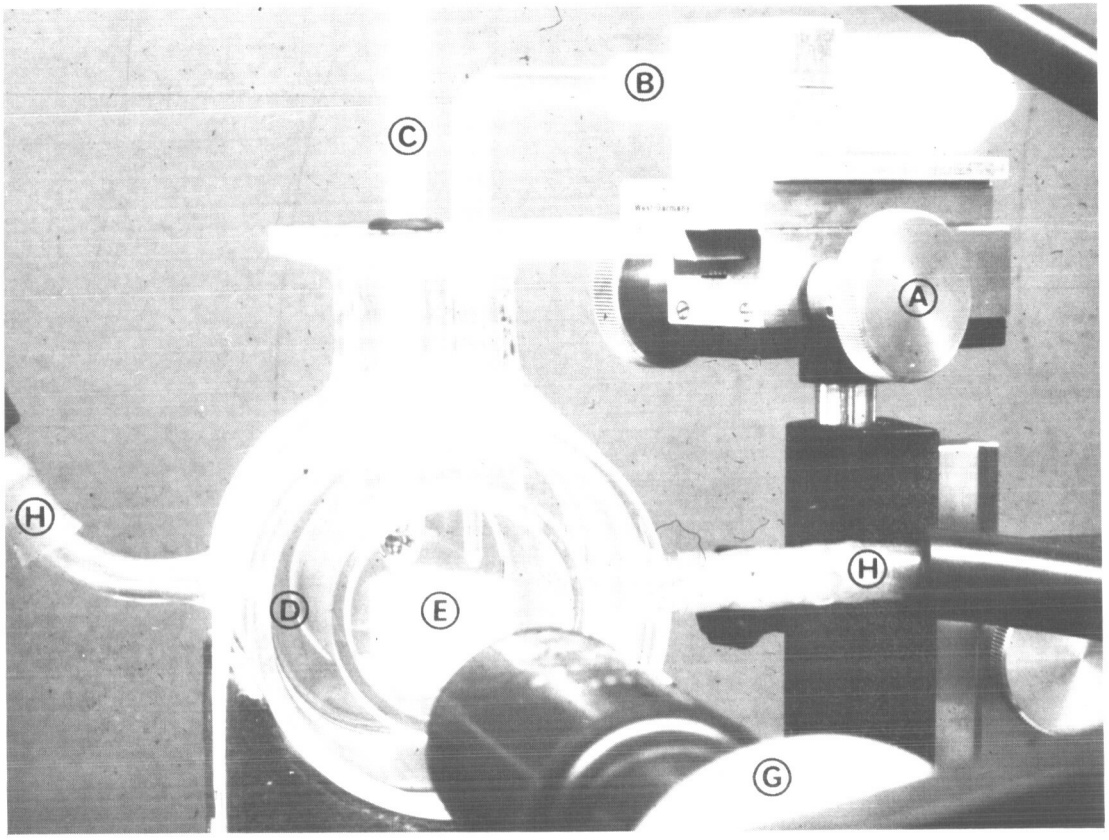

A - Micromanipulator
B - Microsyringe
C - Thermometer
D - Thermostated Cell
E - Polyethylene Planchet
G - Goniometer Telescope
H - Hoses for Circulating Silicone Fluid

FIGURE 3

CRITICAL SURFACE TENSION OF POLISHED DIAMOND

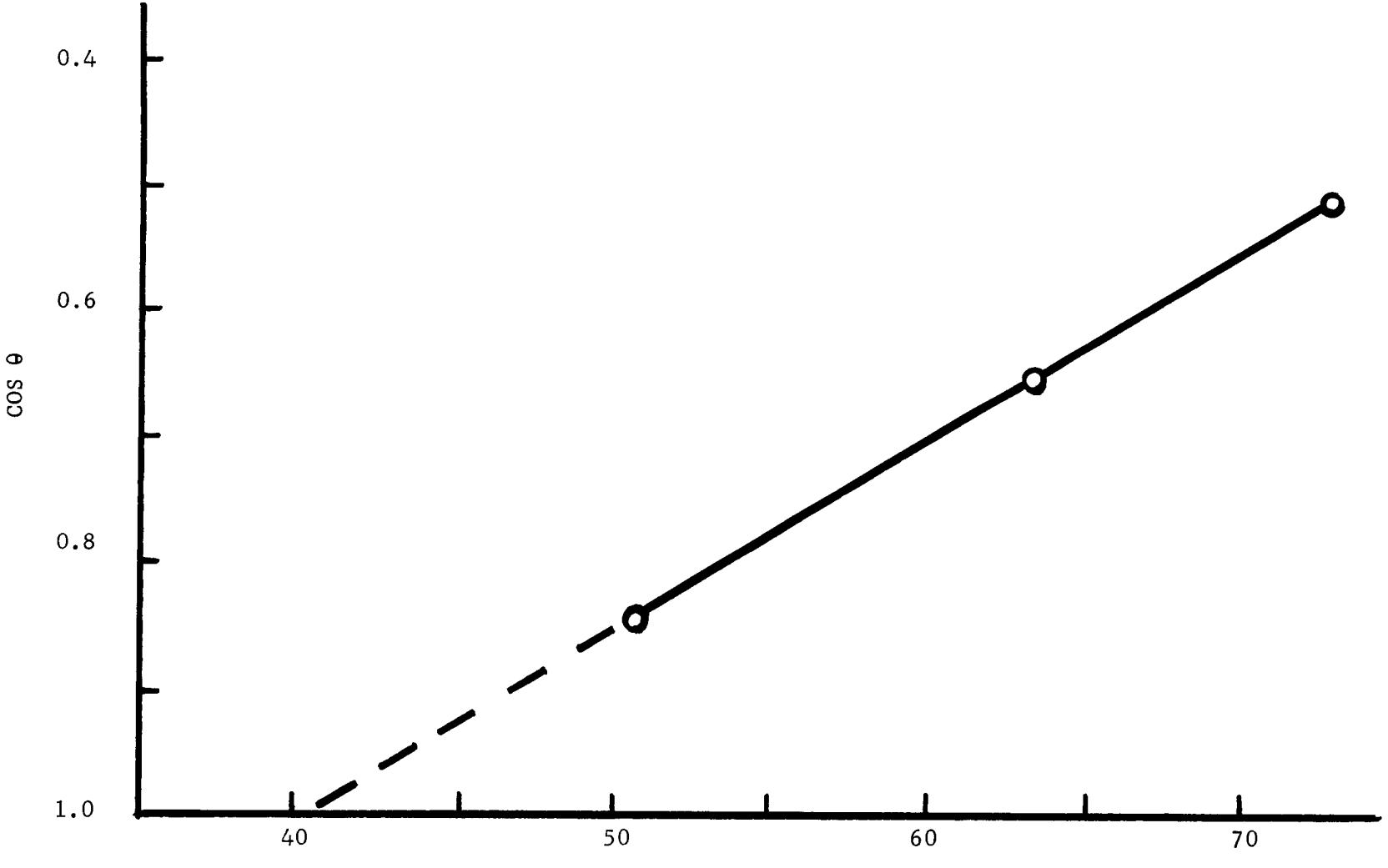

FIGURE 4

Mercury Monolayer/Water/Air Contact Angle Apparatus

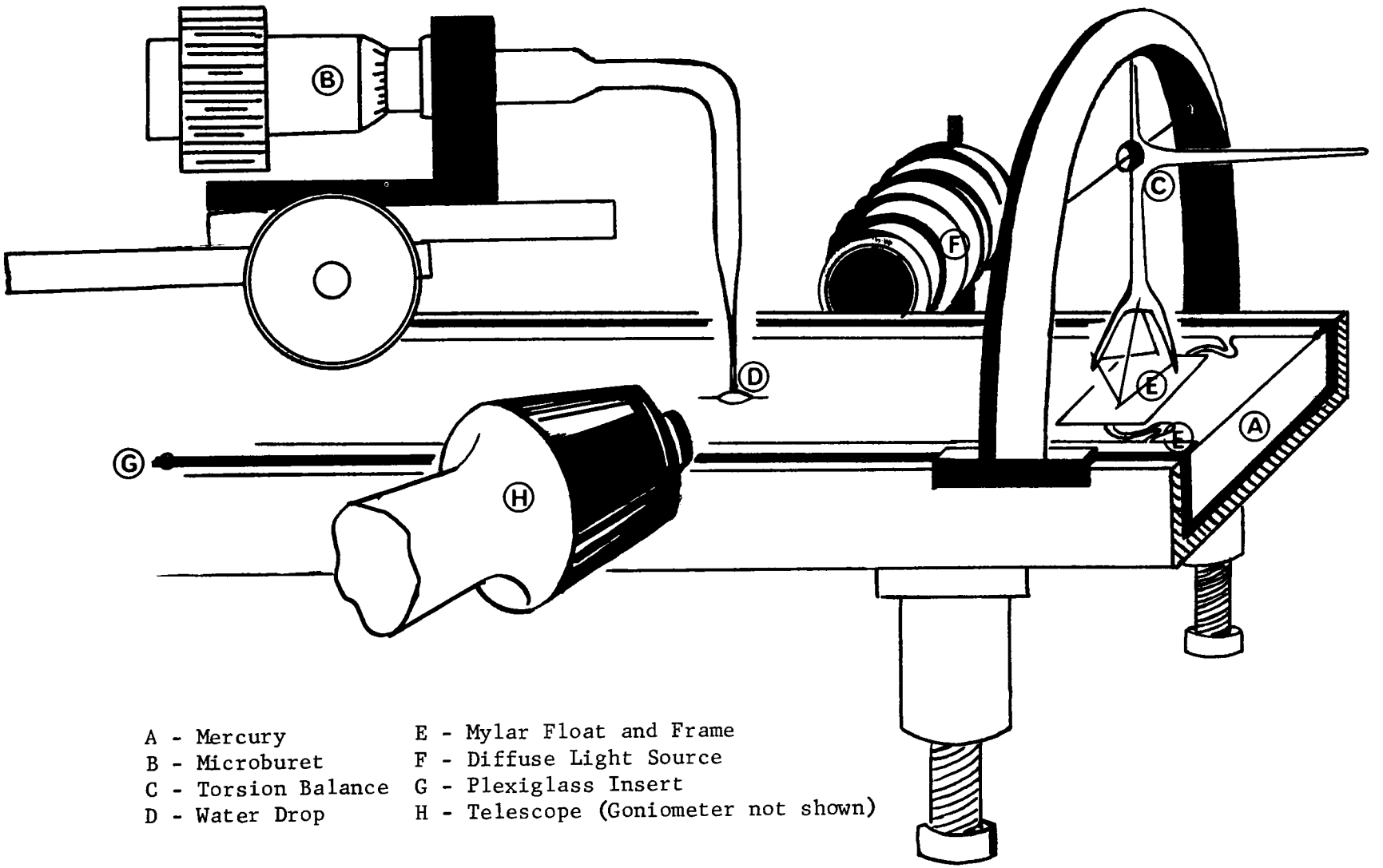

A - Mercury
B - Microburet
C - Torsion Balance
D - Water Drop
E - Mylar Float and Frame
F - Diffuse Light Source
G - Plexiglass Insert
H - Telescope (Goniometer not shown)

FIGURE 5

FILM PRESSURE VS. MOLECULAR AREA
FOR MONOLAYERS ON MERCURY AT 25°C.

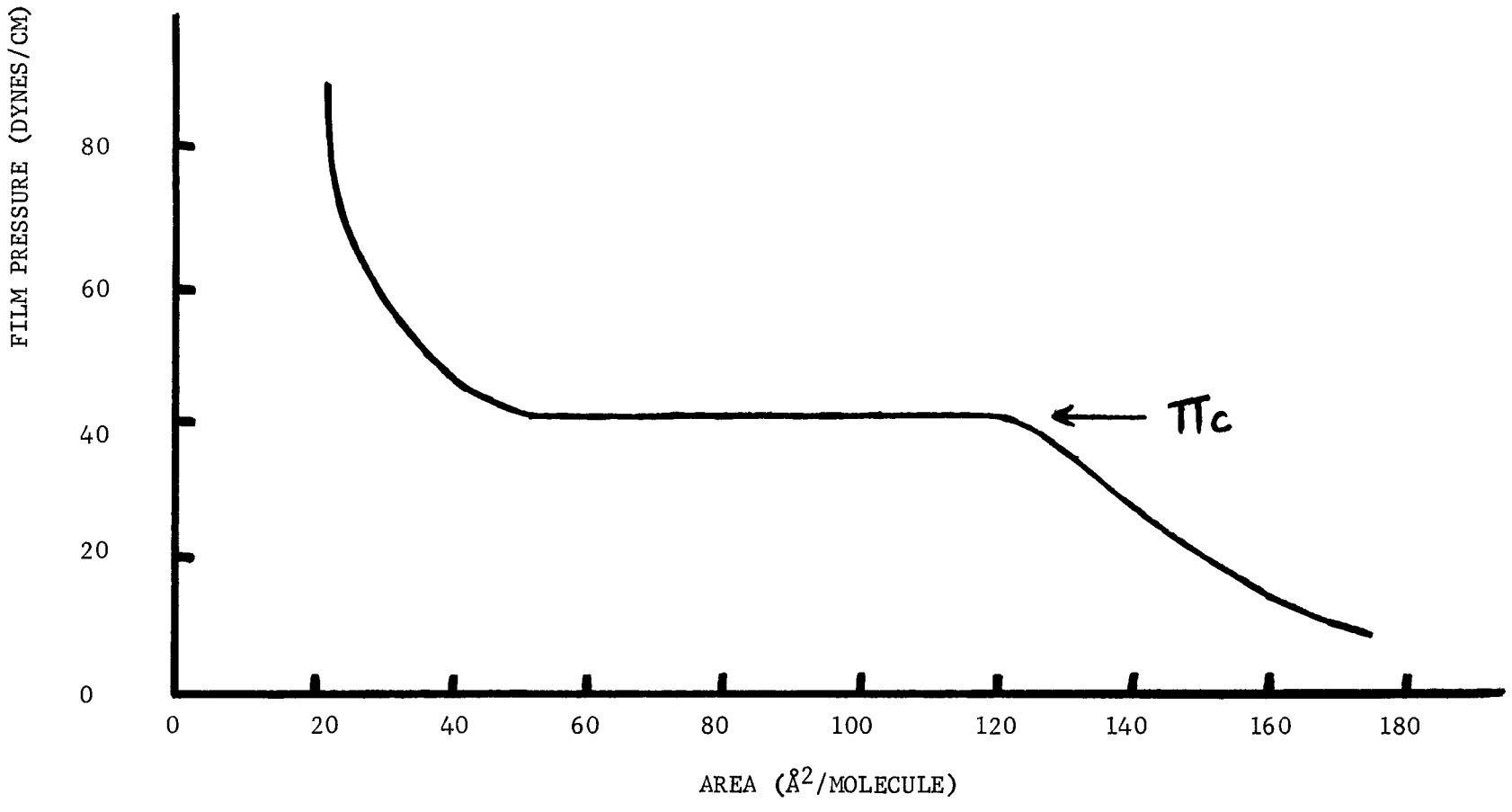

FIGURE 6

Two Possible Cases For A Water Drop On
A Monolayer Covered Mercury Surface at π_c

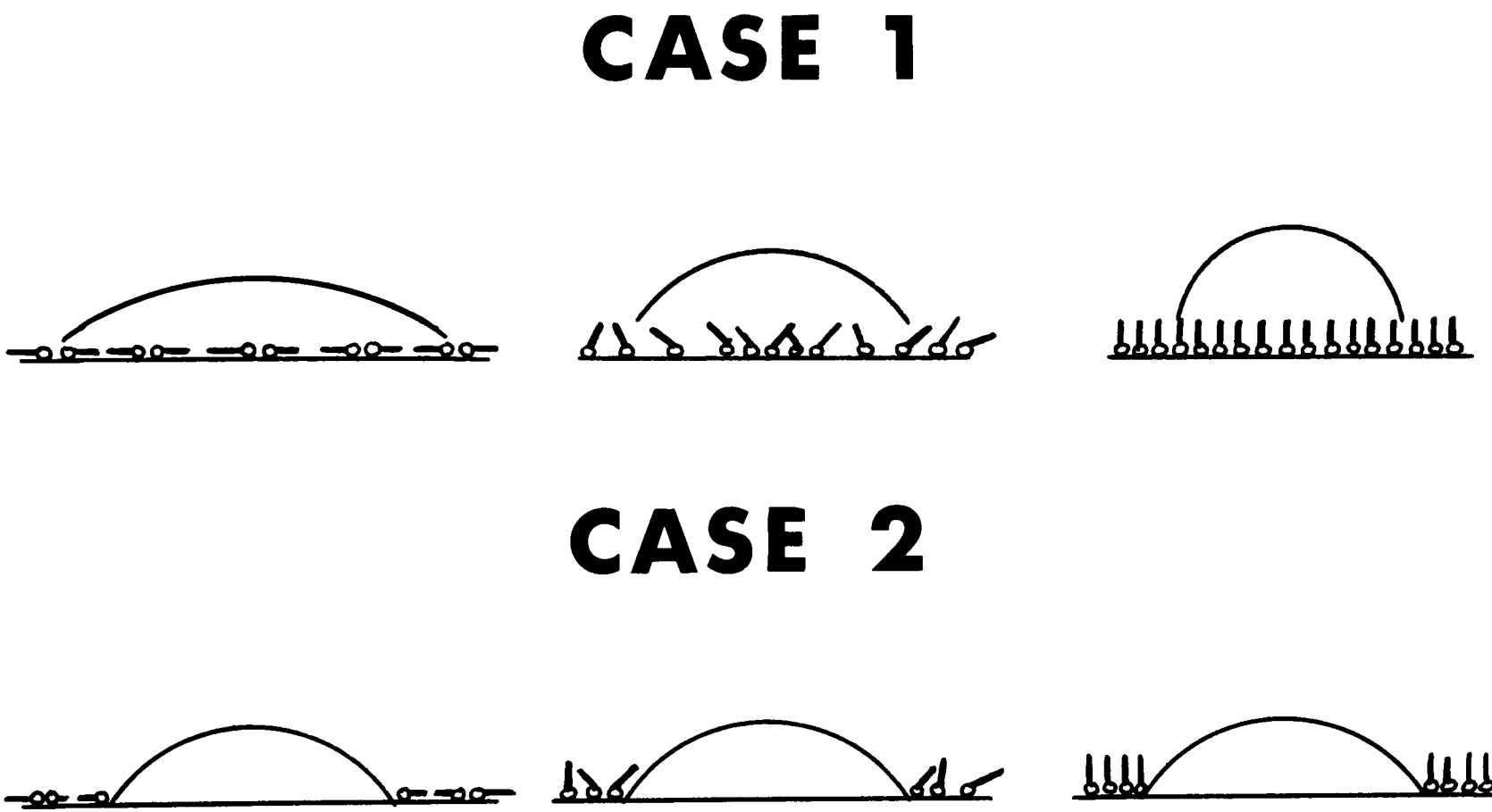

FIGURE 7

COSINE θ VS. FILM PRESSURE AND COSINE θ VS. MOLECULAR AREA FOR WATER ON AN OCTADECANOIC ACID MONOLAYER ON MERCURY AT 25°C.

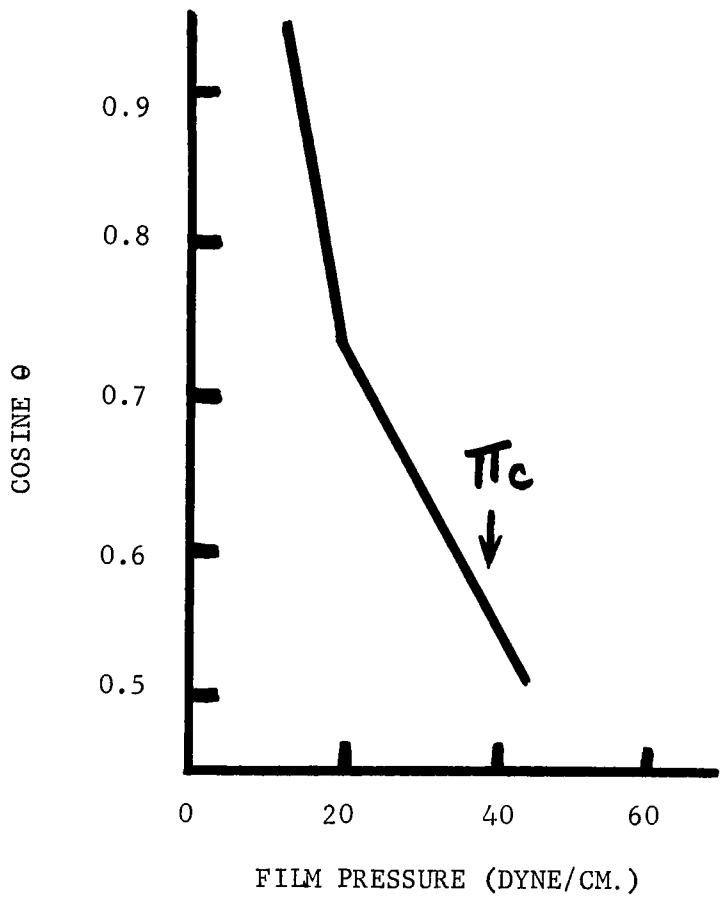

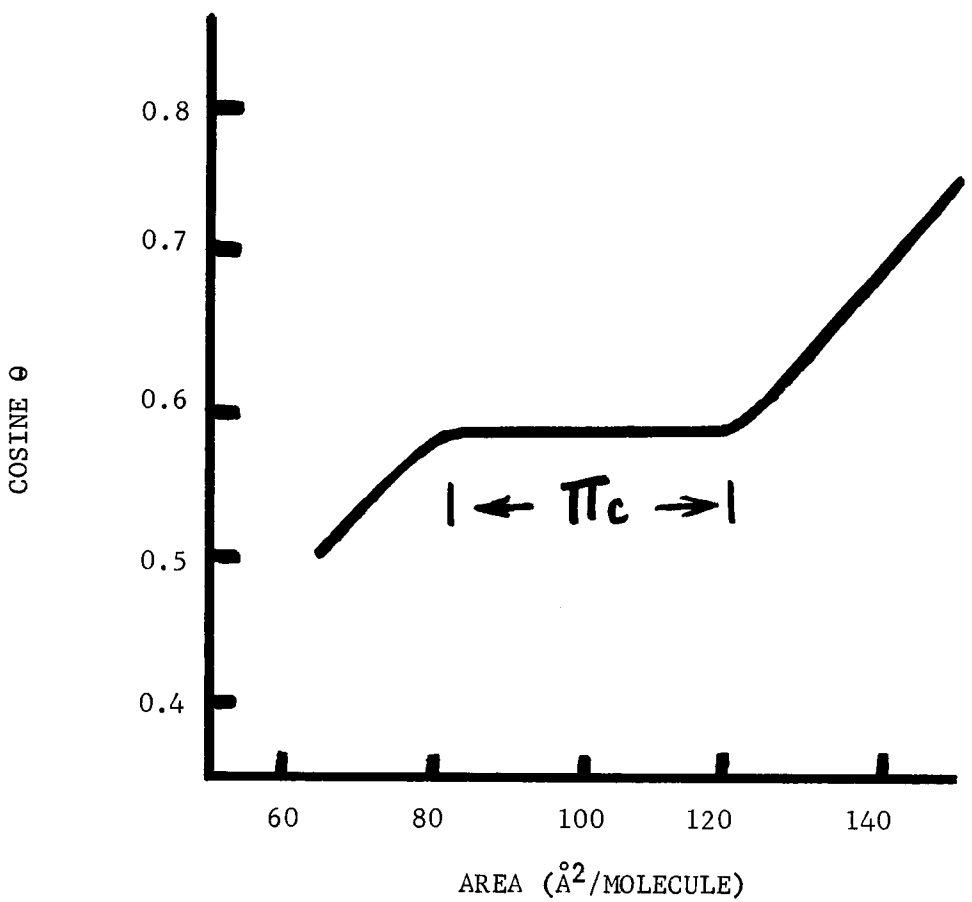

FIGURE 8

COSINE Θ VS. FILM PRESSURE AND COSINE Θ VS. MOLECULAR AREA FOR WATER ON A TETRADECANOIC ACID MONOLAYER ON MERCURY AT 25°C.

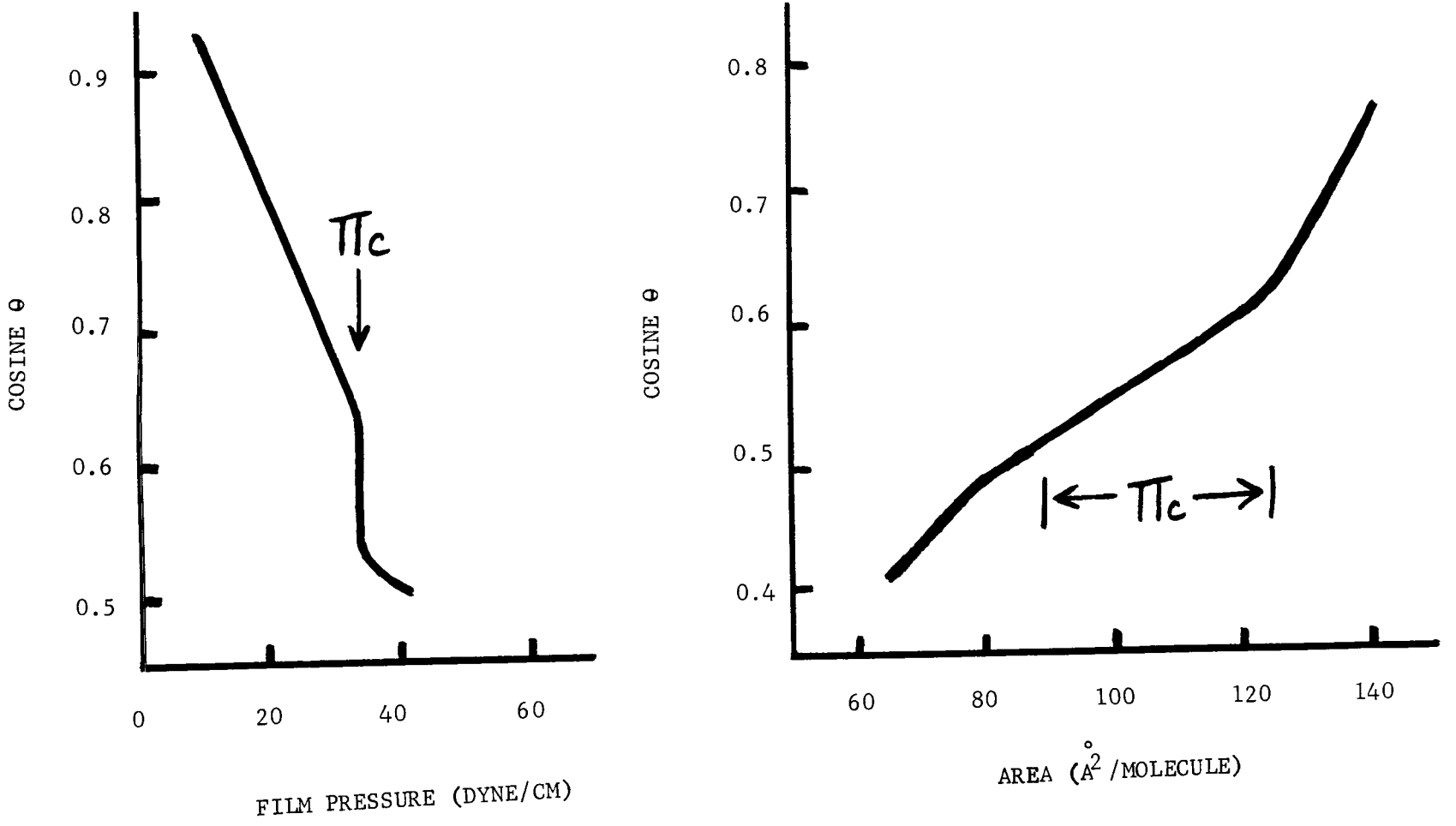

FIGURE 9 - APPARATUS FOR CONTACT ANGLES ON SOLID RARE GASES

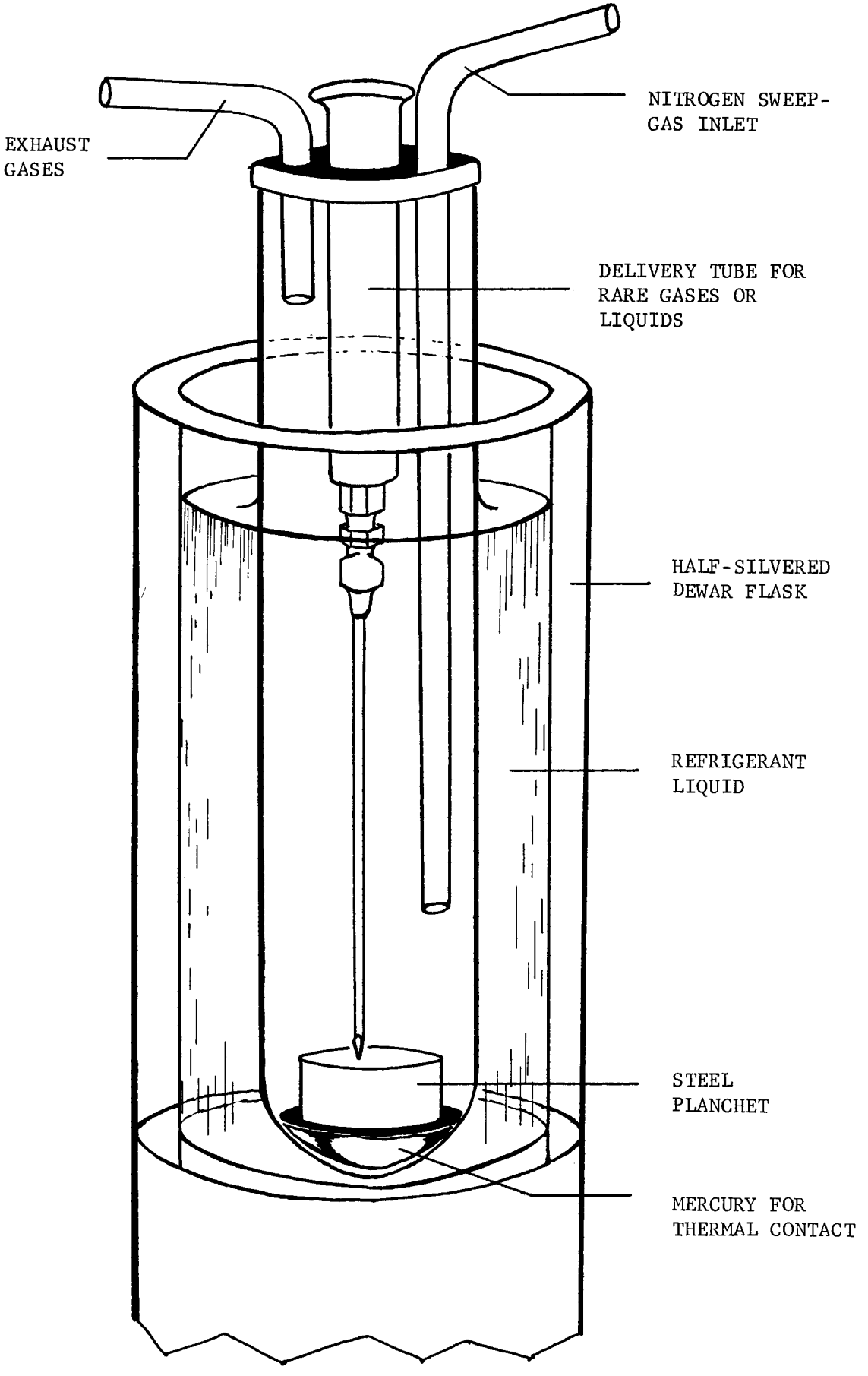

FIGURE 10

Mercury Trough With Surface Potential Electrode

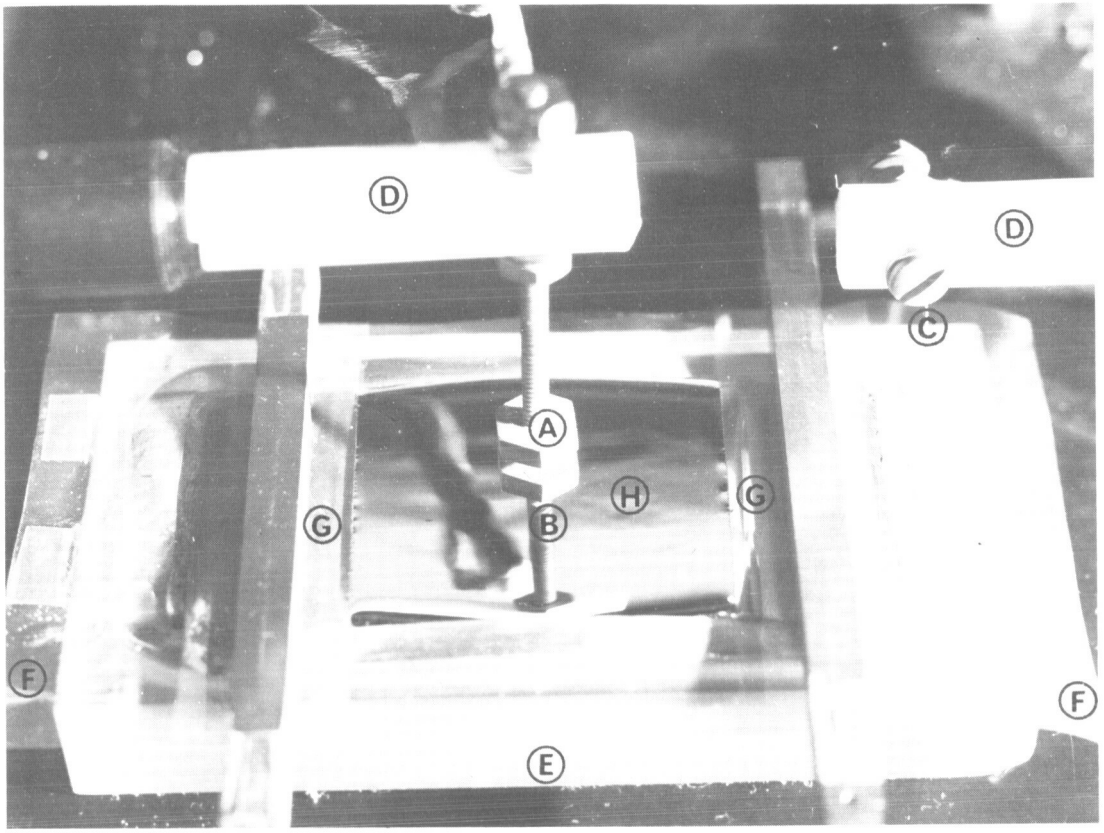

A - Radioactive Electrode
B - Electrode Reflection
C - Platinum Wire
D - "Teflon" Supports
E - Plexiglass Trough
F - Mylar Frame For Trough
G - Mylar Film Barriers
H - Mercury Surface

Figure 11. Effect of Time and Contaminants on Mercury Surface Potential

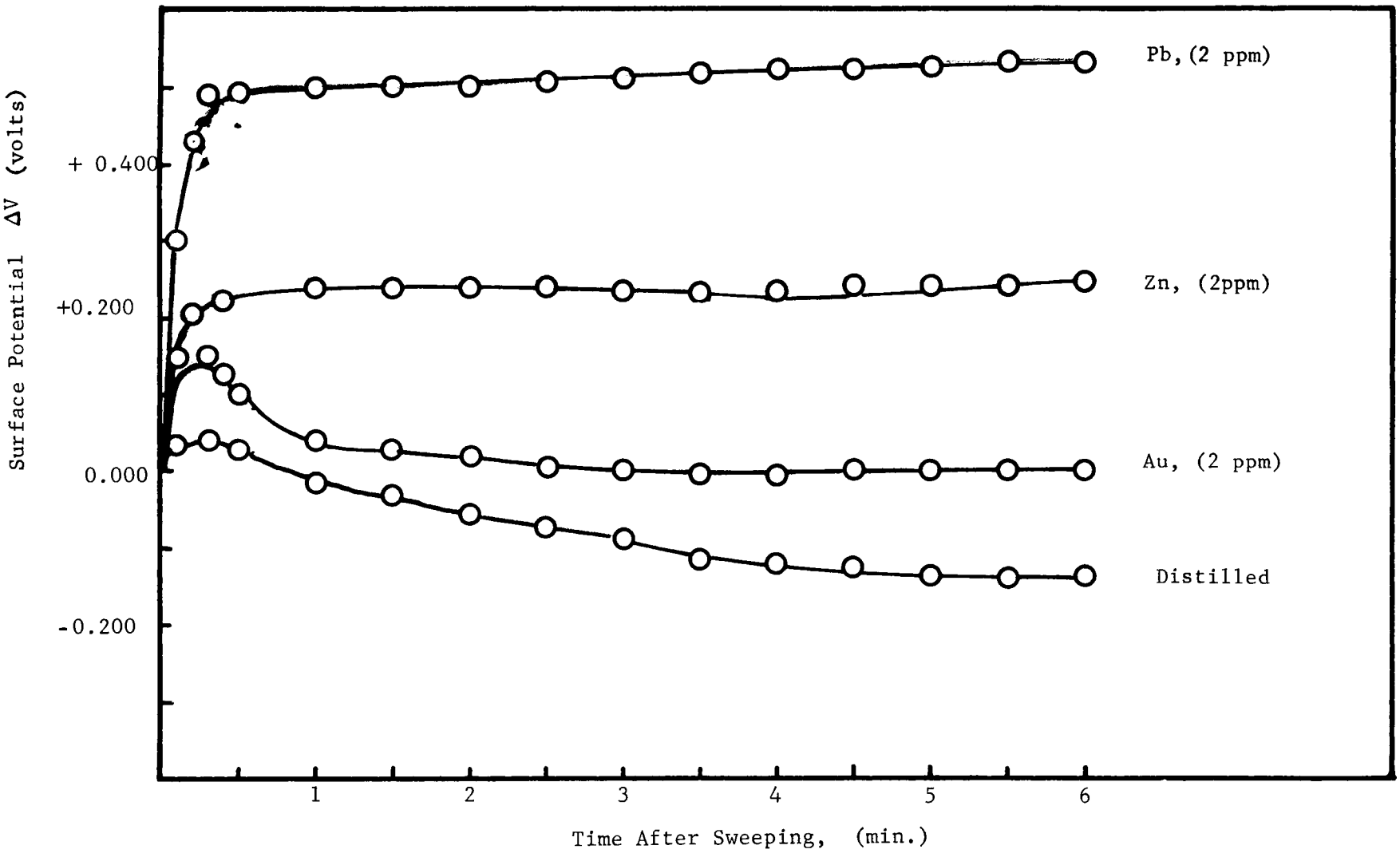

Figure 12. The change in mercury surface potential upon addition of 2 ppm Zn.

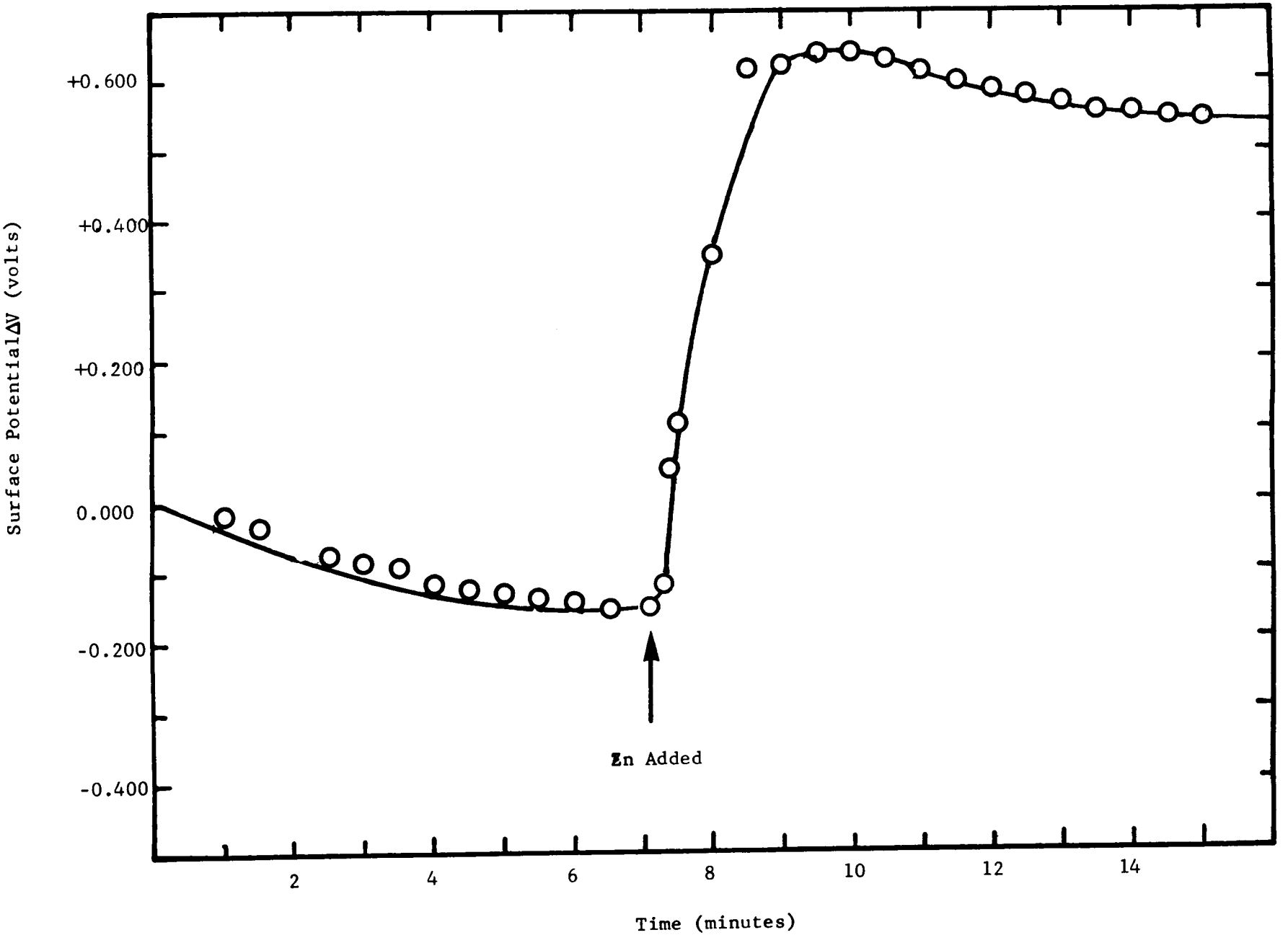

DISTRIBUTION LIST FOR FINAL REPORT

Contract NAS3-8909

	Address	Number of Copies
1.	National Aeronautics and Space Administration Washington, D. C. 20546 Attn: RV-1/Warren Keller	2
2.	NASA-Lewis Research Center 21000 Brookpark Road Cleveland, Ohio 44135	
	Attn: Spacecraft Technology Procurement Section (M.S. 54-2)	1
	Attn: Technology Utilization Office (M.S. 3-19)	1
	Attn: Technical Information Division (M.S. 5-5)	1
	Attn: Library (M.S. 60-3)	2
	Attn: Spacecraft Technology Division	
	a. C. C. Conger (M.S. 54-1)	1
	b. E. W. Otto (M.S. 54-1)	1
	c. D. A. Petrash (M.S. 54-1)	25
	Attn: Report Control Office (M.S. 5-5)	1
3.	NASA Scientific and Technical Information Facility P. O. Box 33 College Park, Maryland 20740 Attn: NASA Representative RQT-2448	6
4.	Southwest Research Institute 8500 Culebra Road San Antonio, Texas 78206 Attn: Dr. H. Norman Abramson	1
5.	Dr. Marvin Adelberg 4043 Cody Road Sherman Oaks, California 91403	1
6.	TRW Space Technology Laboratory One Space Park Redondo Beach, California 90278	
	Attn: Dr. Pravin Bhuta	1
	Attn: Dr. R. E. Hutton	1

	Address	Number of Copies
7.	University of Washington Seattle, Washington 98105 Attn: Dr. C. P. Costello	1
8.	Ball Aerosystems Buffalo, New York 14240 Attn: Minas Insanian	1
9.	University of California Los Angeles, California 90024 Attn: Dr. K. E. Forster	1
10.	Advanced Technology Laboratories General Electric Company Schenectady, New York 12301 Attn: Dr. Novak Zuber Attn: Mr. R. F. Gaertner	1 1
11.	Massachusetts Institute of Technology Cambridge, Massachusetts 02139 Attn: Dr. Peter Griffith	1
12.	Space and Information Systems Div. North American Aviation, Inc. 12214 Lakewood Blvd. Downey, California 90241 Attn: Donald J. Simkin Attn: Dr. Francis C. Hung	1 1
13.	Midwest Research Institute 425 Volker Boulevard Kansas City, Mo. 64110 Attn: Dr. Sheldon Levy	1
14.	Washington State University Pullman, Washington 99163 Attn: Dr. John H. Lienhard	1
15.	University of Michigan Ann Arbor, Michigan 48106 Attn: Dr. John A. Clark Attn: Dr. H. Marca, Jr.	1 1
16.	Astronautics/Propulsion Martin Denver Division Denver, Colorado 80201 Attn: Howard L. Paynter Mail Stop T-14	1

	Address	Number of Copies
17.	Marshall Space Flight Center Huntsville, Alabama 35812	
	Attn: Frank Swalley	1
	Attn: Gordon Platt	1
18.	Spacecraft Thermodynamics Dept. Lockheed Missile & Space Company Sunnyvale, California 94008	
	Attn: Dr. Hugh M. Satterice	1
19.	Manned Spacecraft Center 2101 Webster-Scabrook Road Houston, Texas 77058	
	Attn: Jerry C. Smithson (Mail Stop 2F-21)	1
20.	Mechanical Engineering Dept. Tufts University Medford, Massachusetts 02155	
	Attn: Dr. Lloyd Trefethen	1
21.	NASA-John F. Kennedy Space Center Kennedy Space Center, Florida 32899	
	Mr. J. P. Claybourne/MC	1
22.	Office National E'Etudes Et De Recherches Aerospatinles 29, Avenue de la Division Lecierc 92 Chatillon France	
	Attn: par Michel Delattre	1
	Attn: par Jean Maulard	1
23.	AFWL Firtland Air Force Base, New Mexico	
	Attn: Capt. C. F. Ellis/WLPC	1
24.	Aerospace Corporation P. O. Box 95085 Los Angeles, California 90045	
	Attn: Library Technical Documents Group	1
25.	Westinghouse Astronuclear Laboratories Electric Propulsion Laboratory Pittsburgh, Pennsylvania 15234	
	Attn: H. W. Szymanowski	1